Co(II) COORDINATION NETWORKS BASED ON TWO RIGID DICARBOXYLIC ACIDS: SYNTHESIS, STRUCTURES, AND APPLICATIONS: A LITERATURE OVERVIEW (2005-2015)

Diana Chisca

Institute of Applied Physics, Academy of Science of Moldova, Academiei str. 5, Chisinau, Republic of Moldova
E-mail: chisca.diana.ich@gmail.com

(Received July 14, 2015)

Abstract

Co(II) coordination networks as an integral part of metal-organic materials have been in focus of materials scientists and crystal engineers for the last two decades. This interest stems not only from their reported fascinating architectures and remarkable adsorption properties being the inherent properties of the majority of the so far known metal-organic frameworks, but also from the unique place that Co(II) atom occupies among the transition metals due to its pronounced magnetic properties and colorimetric features. This review highlights the Co(II) mixed-ligand polymeric dicarboxylates built on two rigid dicarboxylic acids, the widely used 1,4-benzenedicarboxylic acid (H_2bdc) and its closest analogue, 4,4'-biphenyldicarboxylic acid (H_2bpdc) that have been reported in the past 10 years. It is focused on: (1) the nature and coordination abilities of Co(II); (2) the synthetic pathways; (3) the impact of size and rigidity of the spacer ligands in the generated coordination networks; (4) examples of one-, two- and three-dimensional coordination polymers; and (5) potential applications of Co(II) coordination polymers.

1. Introduction

Crystal engineering of transition metal complexes, especially coordination polymers (CPs), has been greatly developed in the past decade. Synthesis, characterization, and reactivity of CPs formulated as a coordination compound with repeating coordination entities extending in 1, 2, or 3 dimensions [1], including metal-organic frameworks (MOFs) formulated as a coordination network with organic ligands containing potential voids [1], have been an active research field in recent years. Of great interest are not only the design and synthesis of CPs, but also their enormous variety of intriguing structural topologies, as well as their potential applications in gas sorption, catalysis, luminescence, magnetism, nonlinear optics, and medicine [2, 3]. The most powerful strategy for the architecture of diverse structural topologies in MOFs is the selection of an appropriate multidentate ligand as a linker in connecting metal ions to achieve one-, two-, or three-dimensional network structures [4, 5].

Since 2005, when Co(II)-based MOF-71, Co(bdc)(dmf) and MOF-78, Co(Hpdc)(H_2O)(dmf) (Hpdc=2,7-tetrahydropyrenedicarboxylate) were reported by Yaghi et al. [6], great attention has been paid to coordination chemistry of cobalt complexes with carboxylate

ligands, due to the fact that polynuclear cobalt carboxylates are suitable candidates for structural assembly of new coordination solids with diverse network architectures and useful properties [7]. Thus, in 2009, Zhou and et al. demonstrated that MOF-74-M (M=Mg, Mn, Co, Ni, Zn; MOF-74 = $M_2(dhbdc)(H_2O)_2(H_2O)_{0.6}(EtOH)_{1.6}$, dhbdc=2,5-dihydroxybenzenedicarboxylate), which possess a high concentration of metal open sites, yielded excess storage capacities [8], while among the five isostructural analogues, CoMOF-74 stands ahead for methane and acetylene uptake [9] and exhibits the highest thermodynamic propylene-propane selectivity [10]. Among the indisputable advantages of cobalt ion against other transition metals, stands its diverse coordination capacity with the range of geometries, including the octahedral, tetrahedral, square-pyramidal, trigonal bipyramid, and square-planar ones [11], and its vapochromism [12] since the cobalt-containing MOFs can have a wide range of colors, which makes it easy, in many cases, to identify different phases [13].

The most common intrinsic Co(II) colors are very light pink for octahedral coordination and intense blue for tetrahedral coordination [14]. For distorted octahedral coordination, the pink color can intensify to orange, dark-red, purple, and violet depending on the ligand and the type of distortions. For compounds having both tetrahedral and octahedral coordinated ions, the colors are usually from green to blue depending on the distortions and the ratio of cobalt atoms in the two coordination geometries [15]. This property makes Co(II) coordination networks attractive as chemical sensors [16].

Similar to other MOFs based on transition metals, nowadays the Co(II) coordination networks contain a great many of ligands and expand from the carboxylic networks, including the above-mentioned MOF-71, MOF-78, and CoMOF-74, to the mixed-ligand systems based on the combination of at least two ligands, for example, anionic dicarboxylate and neutral pyridine/bipyridine type ligands [17, 38, 59, 71] or combining both of these functions in one molecule [18]. Based on the information provided by the Cambridge Structural Database (CSD) that now contains data on nearly 700 000 crystal structures [19] it might be stated that carboxylic acids occupy a special place in the Co(II) MOF's crystal engineering, and since it is hard to cover all of them, this overview will be restricted to the reported examples of Co(II) mixed-ligand CPs with two rigid aromatic dicarboxylic acids, 1,4-benzenedicarboxylic acid (H_2bdc) and 4,4'-biphenyl-dicarboxylic acid (H_2bpdc) (Scheme 1), in combination with the neutral ligands summarized in Table 1.

These two ligands, 1,4-benzenedicarboxylic acid (H_2bdc) and 4,4'-biphenyl-dicarboxylic acid (H_2bpdc) (Scheme 1) have been used in the synthetic schemes because they can exhibit a short bridge via one carboxylic group or a long one via the phenyl (biphenyl) moiety which leads to varieties of multi-dimensional MOFs with different kinds of topologies [20].

As bridging ligands, dicarboxylates are of immense interest in the construction of polymeric coordination architectures not only because these polymers have a wide range of structural diversities and potential applications as porous and magnetic materials, but also because dicarboxylates are capable of functioning as hydrogen bond donors and/or acceptors [21].

Table 1. List of ligands with abbreviations

Abbreviations	Ligand	Abbreviations	Ligand
L_1	4,4'-dipyridyl-*N*,*N*'-dioxide	L_{30}	4,4′-*bis*(imidazol-1-yl)diphenylether
L_2	1,2-*bis*(4-pyridyl)hydrazine	L_{31}	1,4-*bis*(imidazol-1-yl)-butane
L_3	2-(4-thiazolyl)benzimidazole	L_{32}	2,2′-dipyridyl-*N*-oxide
L_4	1,4-*bis*-(3-pyridyl)-2,3-diaza-1,3-butadiene	L_{33}	*N*,*N*′-*bis*(3-pyridinyl)-1,4-benzenedicarboxamide
L_5	*N*,*N*′-*bis*-pyridin-4-ylmethylene-hydrazine	L_{34}	3,5-*bis*(4-pyridyl)-1*H*-1,2,4-triazole
L_6	2-(pyridin-3-yl)benzimidazole	L_{35}	4,4'-*bis*(imidazole-yl)biphenyl
L_7	2,8-di(1*H*-imidazol-1-yl)dibenzothiophene	L_{36}	3,5- *bis*(5-(pyridin-4-yl)-4*H*-1,2,4-triazol-3-yl)pyridine
L_8	2-(4-carboxyphenyl)imidazo(4,5-f)(1,10)phenanthroline	L_{37}	*N*,*N*′-*bis*(2-pyridyl)-2,6-diaminopyridine
L_9	2,5-*bis*-(3-pyridyl)-3,4-diaza-2,4-hexadiene	L_{38}	2-(2-pyridyl)-benzimidazole
L_{10}	3-pyridylisonicotinamide	L_{39}	2,2'-bipyridine
L_{11}	1,2-*bis*-[2-(1*H*-1,3-imidazol-1-ylmethyl)phenoxy]ethane	L_{40}	1,4-*bis*(imidazol-l-yl-methyl)-benzene
L_{12}	1-benzylimidazole	L_{41}	4-[*bis*(3,5-dimethyl-3*H*-pyrazol-3-yl)methyl]benzoic acid
L_{13}	2,7-*bis*(ethoxybenzimidazole)-naphthalene	L_{42}	1,6-*bis*(imidazol-1-yl)-hexane
L_{14}	1,5-*bis*(ethoxybenzimidazole)-naphthalene	L_{43}	1,3-*bis*(5,6-dimethylbenzimidazol-1-ylmethyl)benzene
L_{15}	1,3-*bis*(5,6-dimethylbenzimidazol-1-yl)-2-propanol	L_{44}	*N*,*N*′-*bis*-pyridin-4-ylmethylene-naphthalene-1,5-diamine
L_{16}	4-(Hydrazinomethyl)pyridine	L_{45}	dimethylamide
L_{17}	1,4-diazabicyclo[2.2.2]octane	L_{46}	*N*,*N*′-*bis*-4-pyridyl-isophthalamide
L_{18}	1,10-phenanthroline	L_{47}	1,3-*bis*(imidazol-1-yl)benzene
L_{19}	2,7-*bis*(ethoxyimidazole)-naphthalene	L_{48}	3,3′,5,5′-tetramethyl-4,4′-bipyrazole
L_{20}	1,3-*bis*(2-methylbenzimidazol-1-ylmethyl)benzene	L_{49}	1,2-*bis*[2-(2-pyridinyl)ethylidene]hydrazine
L_{21}	2,6-*bis*(imidazole-1-yl)pyridine	L_{50}	3-amino-1,2,4-triazole
L_{22}	4-(4-carboxyphenyl)-2,2,4,4-terpyridine)	L_{51}	4,4'-di(1*H*-imidazol-4-yl)biphenyl
L_{23}	4,4′-bipyridinium-*N*-methyl-4-benzonitrile	L_{52}	1,3-*bis*(2-methylimidazolyl)propane
L_{24}	4,4′-bipyridinium-*N*-methyl-3-benzonitrile	L_{53}	4,4′-(2,5-diethoxy-1,4-phenylene) dipyridine
L_{25}	pyridyl-*N*-oxide	L_{54}	1,4-*bis*(5,6-dimethylbenzimidazol-1-ylmethyl)benzene
L_{26}	4-methylpyridine *N*-oxide	L_{55}	1,1'-*bis*(5,6-dimethylbenzimidazole)methane
L_{27}	3,5-di(pyridine-4-yl)benzoic acid	L_{56}	*N*,*N*,*N*′,*N*′-tetrakis(4-(4-pyridine)-phenyl) biphenyl-4,4'-diamine
L_{28}	1,3-*bis*(4-pyridyl)propane	dma	*N*,*N*-dimethylacetamide
L_{29}	1,3,5-*tris*(pimidazol-ylphenyl)benzene	dmf	*N*,*N*-dimethylformamide

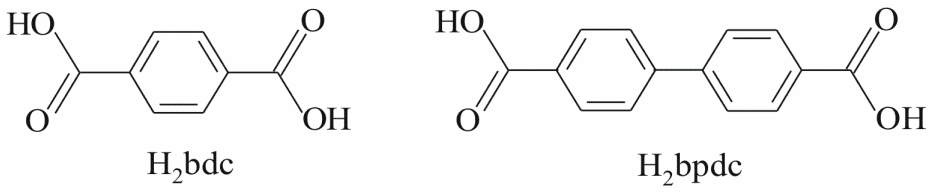

Scheme 1. Structural formulae for dicarboxylic acids with acronyms used in this study.

In this overview, the attempt has been undertaken to summarize the recent progress in design, syntheses, and single crystal structural investigations of Co(II) coordination supramolecular networks based on dicarboxylate aromatic ligands with one and two aromatic rings. The overview covers the works published in the last decade, 2005–2015.

2. Mixed-ligand Co(II) CPs with rigid dicarboxylic acids

Rigid ligands, such as benzene polycarboxylic acids and heterocyclic aromatic compounds, are known as good candidates for assembly in the form of CPs. Among them, historically first was H_2bdc as one of the best spacers for design and construction of MOFs, due to the equally spaced carboxylate groups, rigidity of the phenyl skeleton and especially its various bridging abilities [22].

The statistical analysis of Co(II) CPs with aromatic dicarboxylic acids, such as phenyl and biphenyl dicarboxylic acids, has been undertaken based on the data extracted from the Cambridge Structural Database (CSD, version 1.17, 2015) and from the current scientific sources (Fig. 1). It has been revealed that Co(II) coordination networks only with H_2bdc and H_2bpdc have been reported so far.

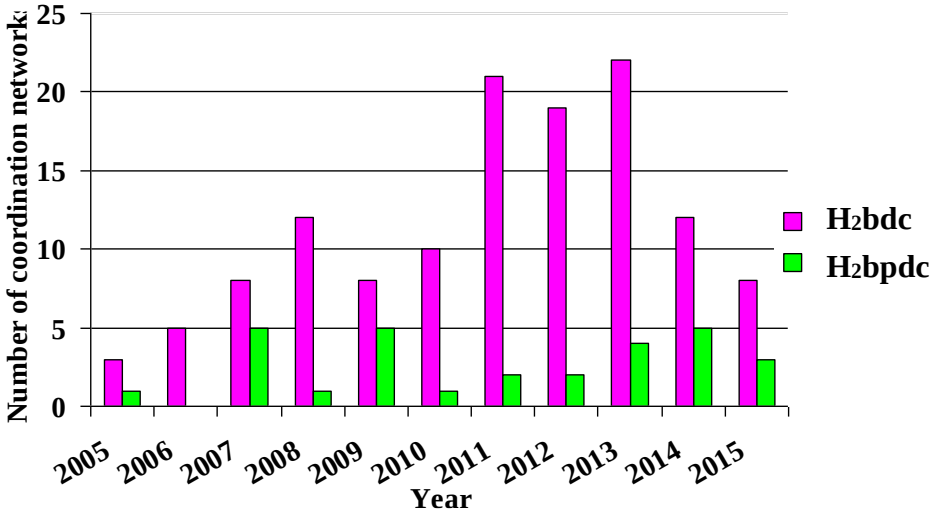

Fig. 1. Histogram with distribution of Co(II) CPs with aromatic dicarboxylic ligands.

2.1 Synthesis

Four main synthetic strategies (saturation, diffusion, hydro(solvo)thermal, microwave and ultrasonic methods) for obtaining CPs are extracted from the literature [23] and summarized in Tables 2 and 3 for H_2bdc and H_2bpdc, respectively. Improvement of synthetic procedure is essential in order to obtain high-quality single crystals suitable for X-ray measurements. It is widely documented that the structure and topology of CPs generated from transition metals and organic ligands can be controlled by the selection of ligands, pH of the

reaction medium, solvents, metal ions, metal-to-ligand ratios, reaction temperature, counterions, and so forth [3, 5]. In particular, solvent nature is an important factor since its structure, as well as chemical properties, can influence the rate of crystal growth and the final structure. A large number of new MOFs have been constructed in the presence of the templating molecules showing unprecedented structural characteristics and, in some cases, solvent-induced properties, such as enhancement of porosity [24], electrochemical property [25], catalytic activity [26], and so forth. The CPs are generally synthesized in the liquid phase by using a solvent as a medium to induce the self-assembly of a regular framework. The reaction can be carried out by mixing a solution of metal ions with a solution of ligands at room temperature or under hydrothermal/solvothermal conditions (where one or all components are poor soluble compounds) [27]. For example, compounds $[Co(bdc)(pyz)]_n$ and $\{[Co(bpdc)(2,2'\text{-bpy})(H_2O)]_n \cdot nH_2O\}_n$ (where pyz = pyrazine, 2,2'-bpy=2,2'-bipyridine) were prepared under hydrothermal conditions at high temperatures of 120–200ºC in a neutral or slightly acid medium [28]. The $\{[Co_2(bdc)_2(ted)] \cdot 2dmf \cdot 3H_2O\}_n$ compound (where ted=triethylenediamine) was prepared by the layered-solution method using $CoCl_2$, triethylenediamine, and H_2bdc in DMF and methanol solvents as starting materials [29]. The $\{[Zn_2Co(bpdc)_3(dmf)_2] \cdot 4dmf\}_n$ complex was prepared via solvothermal synthesis from mixtures of the respective transition metal salts and H_2bpdc [30].

2.2. Mode of coordination

Dicarboxylates are widely used in the supramolecular assembly as mono-, bi- or multi-dentate ligands because they can adopt a variety of coordination modes to the metal centers. The generalizations reported herein are made on the CSD statistics for the cobalt(II) ion coordination modes in the polymeric dicarboxylates and based on the Harris notation [31] (Scheme 2).

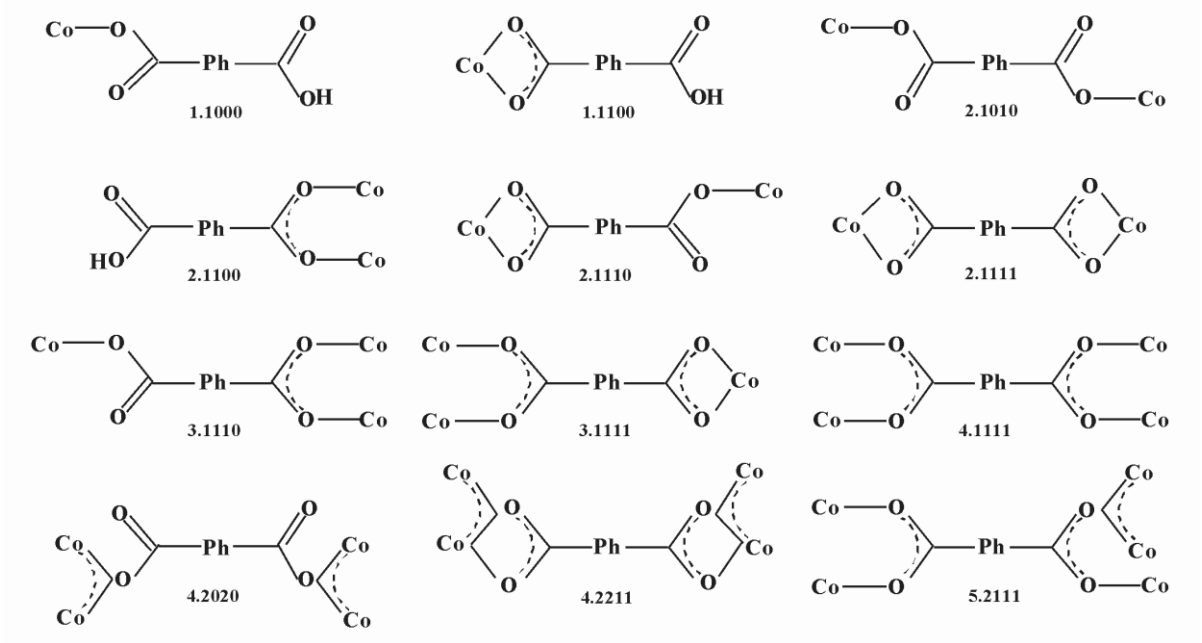

Scheme 2. Crystallographically established modes of carboxylate coordination to the Co(II) metal atoms.

2.3. Dimensionality of polymeric Co(II) dicarboxylates

The organization of the building blocks together can lead to CPs of different dimensionalities, such as one-, two-, or three-dimensional architectures. In order to illustrate the wide diversity of Co(II) CPs with dicarboxylic acids, some examples are given. They are classified along with their dimensionalities, and our retrieval of the CSD revealed 171 hits of H_2bdc ligand with Co(II) metal, 17 of which are one-dimensional (1D), 32 are two-dimensional (2D), and 65 are three-dimensional (3D) networks, while of 35 hits with H_2bpdc ligand 3 are 1D, 7 are 2D, and 25 are 3D CPs (Fig. 2). The CPs will be further discussed in the hierarchy of increase in their dimensionality (Tables 2, 3). The Figures were reproduced by Mercury facilities [32] using cif files extracted from CSD.

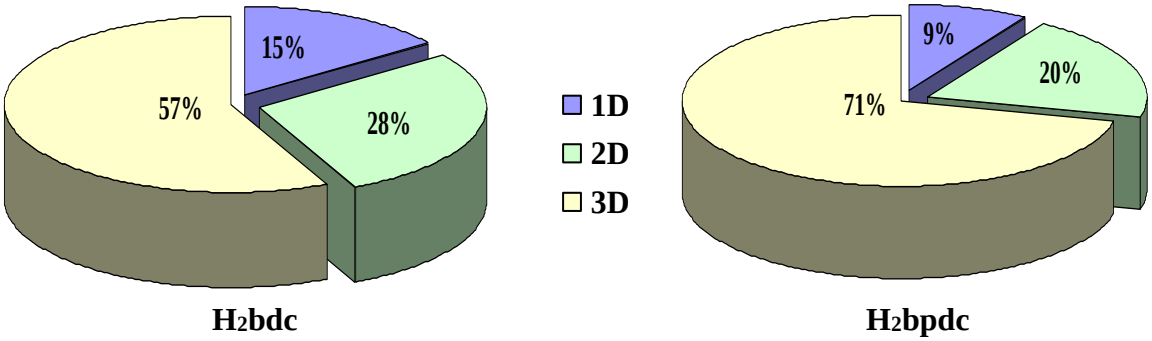

Fig. 2. Histograms with distribution of Co(II) CPs with aromatic dicarboxylic ligands against dimensionalities.

2.3.1. CPs of Co(II) with 1,4-benzenedicarboxylate

2.3.1.1. One-dimensional motifs

The selected 1D arrays are shown in Fig. 3. The crystals of $[Co(bdc)(L_6)_2(H_2O)_2]_n$, were obtained by the hydrothermal synthesis. The compound crystallizes as the linear chain shown in Fig. 3a where the Co(II) atoms are bridged by the monodentate-coordinated bdc anions to form 1D benzenedicarboxylate-bridged polymeric chain structure. The Co(II) atoms are in N_2O_4 octahedral environment [33].

The formation of the zig-zag chains can be induced by the chelate mode of coordination of N-ligand molecules. The zig-zag structure of the $[Co(bdc)(L_3)]_n$ compound, which is shown in Fig. 3b, is provided by the bulky $[Co(II)(L_3)]^{2+}$ corner fragment; each cobalt atom adjusts the distorted N_2O_4-octahedral environment; both carboxylic groups of the bdc ligands act in a bidentate bridging mode [34].

From slow diffusion techniques in a water-methanol medium, crystals of $\{[Co(L_1)(bdc)(H_2O)_2]\cdot[Co(H_2O)_6]\cdot(bdc)\cdot(H_2O)\}_n$ were obtained [35]. The polymeric chain is formed by almost collinear hexacoordinated Co(II) ions in the O_6-octahedral environment doubly bridged by a bdc carboxylate group and a L_1 oxygen. The crystal packing shows bdc dianions and water molecules inserted in between the ribbons (Fig. 3c).

Ladder-like 1D motifs can also be formed. An example is shown in Fig. 3d. In the $\{[Co_2Br_2(bdc)(L_2)_2]\cdot 4dma\cdot 2H_2O\}_n$ compound [36], the tetrahedral Co(II) ions are coordinated with three different ligand molecules. These Co^{2+} ions are connected by bidentate L_2 ligands to form a 1D wavy chain. Two chains are bridged together by ditopic bdc^{2-} ligands as rungs into a molecular ladder.

Table 2. Selected examples for Co(II)-1,4-benzenedicarboxylate CPs

Composition [a]	Method of synthesis	Color	Coordination number of Co(II)	Dimensionality	Reported properties	Reference, refcode in CSD
$\{[Co(bdc)(L_1)(H_2O)_2]\cdot[Co(H_2O)_6]\cdot bdc\cdot H_2O\}_n$	slow diffusion	red	6	1D	magnetism	[35] QEYZOK
$\{[Co_2(bdc)Br_2(L_2)_2]\cdot 4dma\cdot 2H_2O\}_n$	hydrothermal	red	4	1D	adsorption	[36] FEFFED
$[Co(bdc)(L_3)]_n$	hydrothermal	red	6	1D	–	[34] NIFSUS
$\{[Co(bdc)_2(H_2O)_2(L_4)_2Co(H_2O)_4]\cdot 6H_2O\}_n$	room temperature	red	6	1D	–	[78] QOMTOD
$\{[Co(bdc)_2(L_5)_3(H_2O)_4]\cdot 2CH_3OH\cdot 3H_2O\}_n$	room temperature	red	6	1D	–	[79] ZOHQEU
$[Co(bdc)(L_6)_2(H_2O)_2]_n$	hydrothermal	red	6	1D	–	[33] CODZOM
$\{[Co(bdc)(L_7)]\}_n$	hydrothermal	colorless	4	2D	–	[80] TONPUJ
$\{[Co_2(bdc)(L_8)_2]\cdot 4nH_2O\}_n$	hydrothermal	yellow	6	2D	catalysis	[67] DIMXAA
$[Co(bdc)(L_9)(H_2O)_2]_n$	room temperature	red	6	2D	–	[78] QOMTUJ
$[Co(bdc)(L_{10})_2]_n$	hydrothermal	purple	6	2D	–	[81] EGATEN
$\{[Co(bdc)(L_{11})]\cdot 2H_2O\}_n$	hydrothermal	red	6	2D	–	[39] APOKEW
$[Co_2(bdc)_2(L_{12})_4]_n$	room temperature	red	6	2D	luminescence	[38] BOFGOT
$\{[Co(bdc)(L_{13})]\cdot H_2O\}_n$	hydrothermal	red	6	2D	luminescence	[69] GOPCEV
$\{[Co(bdc)(L_{14})(H_2O)]\cdot 2dmf\}_n$	hydrothermal	red	6	2D	luminescence	[69] NOHBOD
$[Co(bdc)(L_{15})]_n$	hydrothermal	red	4	2D	catalysis	[82] HINTEF
$Co\{[bdc]_{0.5}[Hbdc][L_{16}]\}_n$	hydrothermal	dark red	6	2D	gas storage	[42] CIDDEA
$[Co(bdc)(L_4)(H_2O)_2]_n$	hydrothermal	red	6	2D	–	[37] SODXIU
$[Co_2(bdc)_2(L_{17})]_n$	desorption	purple	5	2D	gas storage	[60] TONXIE
$[Co_3(bdc)_2(N_3)_2(L_{18})_2]_n$	hydrotermal	purple	5	2D	magnetism	[83] IBISAP
$\{[Co(bdc)(L_{19})(H_2O)_2]\cdot H_2O\}_n$	hydrothermal	yellow	6	2D	luminescence	[84] GOPCAR
$[Co(bdc)(L_{20})]_n$	hydrothermal	pink	4	2D	fluorescence and catalytic	[95] XUBRAP
$[Co(bdc)(L_{21})]_n$	solvothermal	pink	4	2D	–	[96] XUDVEZ
$[Co_3(bdc)_3(dmf)_2(H_2O)_2]_n$	heating and stirring	purple	6	2D	catalytic activity	[97] DUCQUP
$[Co_2(bdc)(L_{22})_2(H_2O)]_n$	solvothermal	pink	6	3D	catalysis	[85] DOJXEH
$\{[Co_4(bdc)_3(N_3)_4(L_{23})_2]\cdot 2nH_2O\}_n$	hydrothermal	darkpurple	6	3D	magnetism	[69] KIYCEC

Table 2. (*continued*)

Composition [a]	Method of synthesis	Color	Coordination number of Co(II)	Dimensionality	Reported properties	Reference, refcode in CSD
$\{[Co_4(bdc)_3(N_3)_4(L_{24})_2]\cdot nH_2O\}_n$	hydrothermal	black	6	3D	magnetism	[69] KIYCEC
$[Co(bdc)(L_{25})]_n$	hydrothermal	pink	6	3D	magnetism	[72] NIKFEU
$[Co(bdc)(L_{26})]_n$	hydrothermal	pink	6	3D	magnetism	[72] YITMEV
$\{[Co_2(bdc)(L_{27})_2(H_2O)]\cdot 2H_2O\cdot 6dmf\}_n$	hydrothermal	red	6	3D	magnetism	[73] TIXKUI
$\{[Co_2(bdc)_2(L_1)]\cdot H_2bdc\cdot 2MeOH\}_n$	solvothermal	red	6	3D	magnetism, gas storage	[74] ADAXEK
$\{[Co_2(bdc)_2(L_1)]\cdot 2dmf\}_n$	solvothermal	red	6	3D	magnetism, gas storage	[74] ADAXIO
$\{[Co(bdc)(L_{28})]_4\cdot 6H_2O\}_n$	hydrothermal	purple	4	3D	–	[75] BIYFAR
$\{[Co_6(bdc)_2(L_{29})(SO_4)]\cdot 7dmf\}_n$	hydrothermal	blue	4	3D	reversible SC-SC transformation	[61] GINPAW
$\{[Co_3(L_{29})(SO_4)\text{-}(H_2O)_{7.2}(bdc)]\cdot(solvent)\}_n$	exposed to air	red	6	3D	reversible SC-SC transformation	[61] GINPAW
$\{[Co_2(bdc)_2(L_{17})]\cdot 2dmf\cdot 3H_2O\}_n$	layered-solution	blue	5	3D	desorption	[29] DIZVAK
$\{[Co(bdc)(L_{30})]_2\cdot 2H_2O\cdot dmf\}_n$	hydrotermal	coloress	5	3D	photochemistry	[76] OKIPOO
$[Co(bdc)(L_{18})(H_2O)]_n$	hydrotermal	brown	5	3D	luminescence	[77] RAMHES 02
$[Co(bdc)(L_{31})_{0.5}]_n$	hydrotermal	dark purple	6	3D	magnetism	[98] GOZTEW
$[Co_2(bdc)_2(L_{32})]_n$	solvothermal	pink	6	3D	gas adsorption	[99] LOVVAV
$[Co_3(bdc)_3(L_{32})_2]_n$	solvothermal	pink	6	3D	gas adsorption	[99] LOVVEZ
$[Co_3(bdc)_3(L_{33})]_n$	hydrotermal	pink	5,6	3D	magnetism	[100] DOYMUB
$\{[Co_2(bdc)_2(L_{34})_2]\cdot 2H_2O\}_n$	hydrotermal	red	6	3D	magnetism	[101] ROWVOQ
$\{[Co_2(bdc)_2(L_{34})_2]\cdot H_2O\cdot MeOH\}_n$	hydrotermal	purple	5,6	3D	magnetism	[101] ROWVUW
$[Co(bdc)(L_{35})]_n$	solvothermal	purple	4	3D	–	[102] UHOFEE
$[Co(bdc)L_{36}\cdot 2dmf]_n$	solvothermal	red	6	3D	electrochemical, sorption, galvanostatic charge-discharge	[103] YUBTIA

[a] For L_1-L_{36} ligands' names, see Table 1.

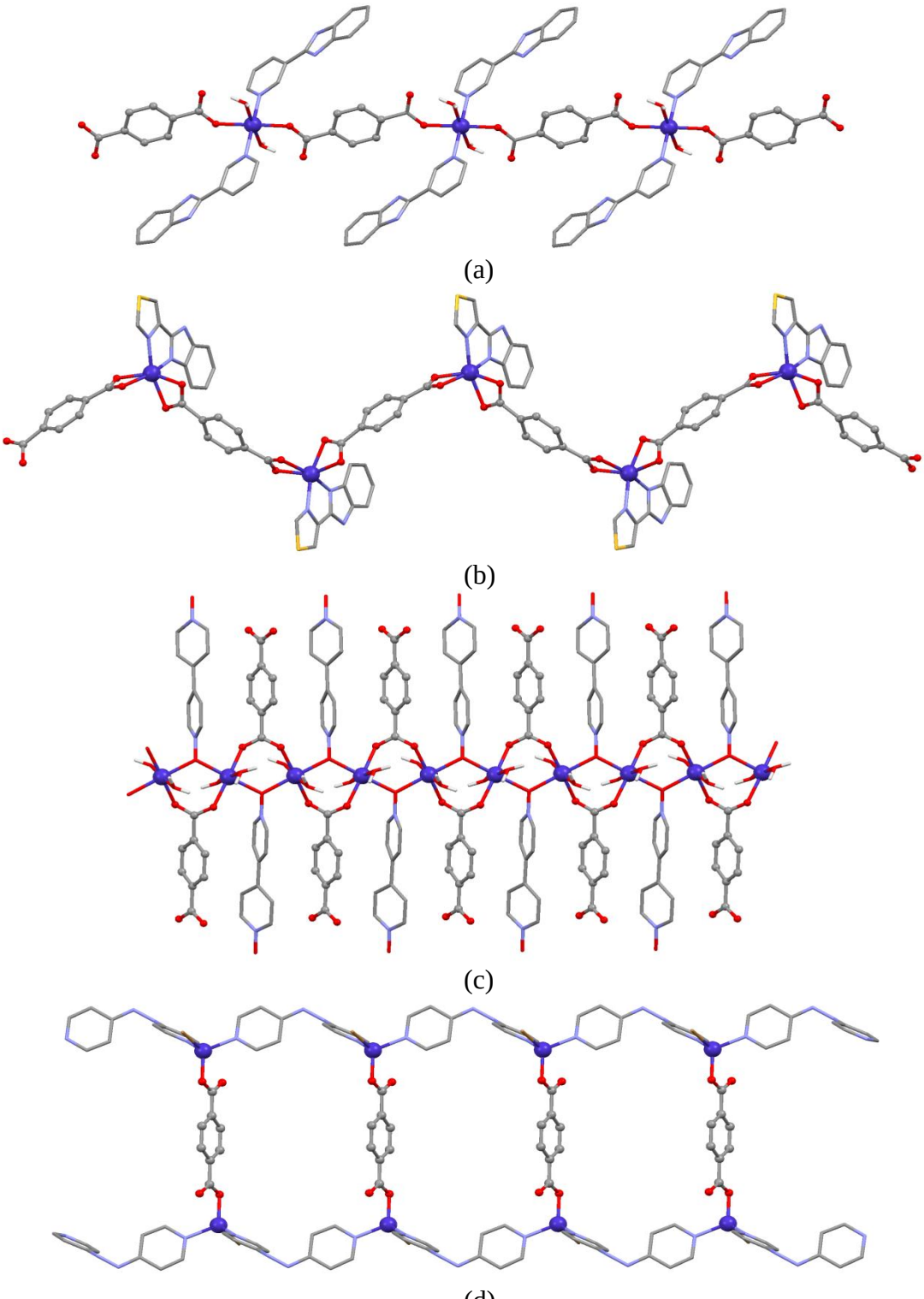

(a)

(b)

(c)

(d)

Fig. 3. 1D coordination arrays: linear chain in *catena*-[(μ_2-terephthalato)-*bis*(2-(pyridin-3-yl)-1*H*-benzimidazole)-diaqua-cobalt(II)] (a) [33], zig-zag chain in *catena*-((μ_2-terephthalato)-(2-(1,3-thiazol-4-yl)-1*H*-benzimidazole)-cobalt(II)) (b) [34], ribbon in *catena*-((μ_2-terephthalato-*O*,*O'*)-(μ_2-4,4'-bipyridine-*N*,*N'*-dioxide-*O*,*O'*)-diaqua-cobalt(II) hexa-aqua-cobalt(II) terephthalate monohydrate) (c) [35], and ladder in *catena*-((μ_2-terephthalato)-*bis*(μ_2-4,4'-hydrazine-1, 2-diyldipyridine)-dibromo-di-cobalt(II)) (d) [36].

2.3.1.2. Two-dimensional motifs

Square grid networks are the simplest examples of the 2D motifs. In these CPs, the metal to ligand proportion is usually 1 : 2. The metal centers are coordinated with four different ligand molecules, and the repetition of this unit allows the propagation of the structure in two dimensions.

Thus, in compound $[Co(bdc)(L_{17})(H_2O)_2]_n$, the metal ions have an octahedral environment: the equatorial positions are occupied by two bdc^{2-} anions and two water oxygen atoms, and the axial positions are occupied by two nitrogen atoms from two L_{17} molecules [37]. Further expansion of the structure through the monodentate bridging bdc^{2-} anions and L_{17} ligands creates a (4,4) rhomboidal layer grid (Fig. 4a).

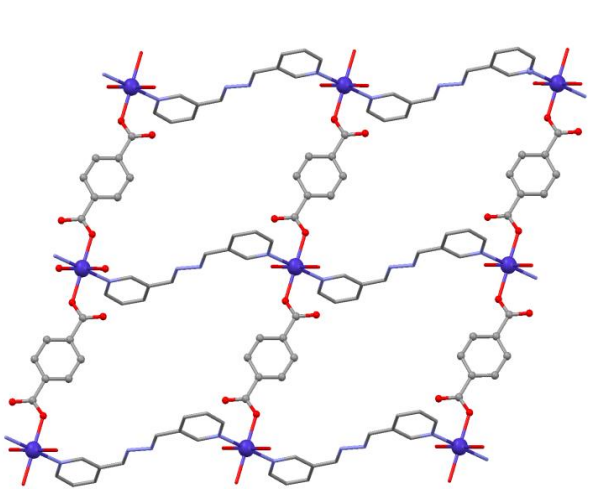

(a)

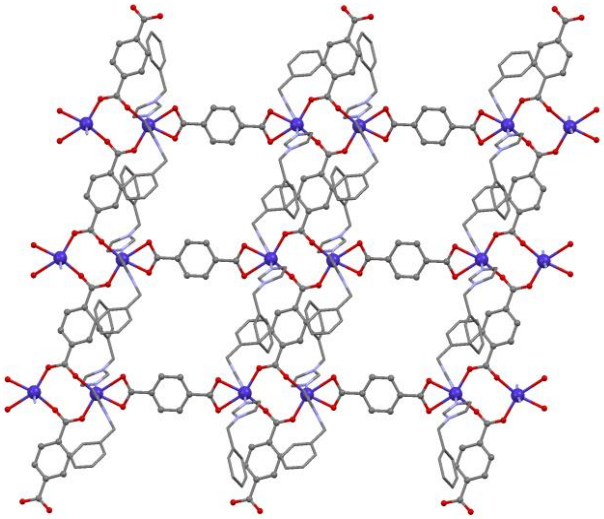

(b)

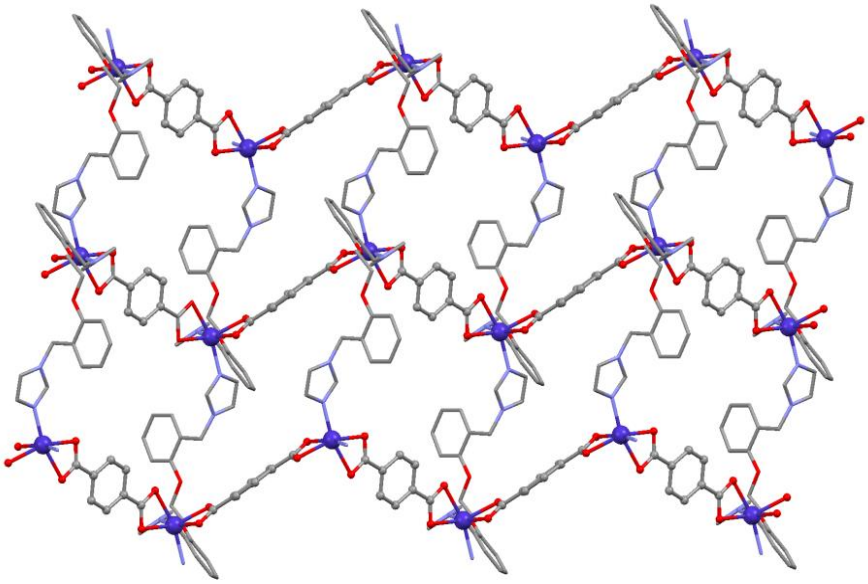

(c)

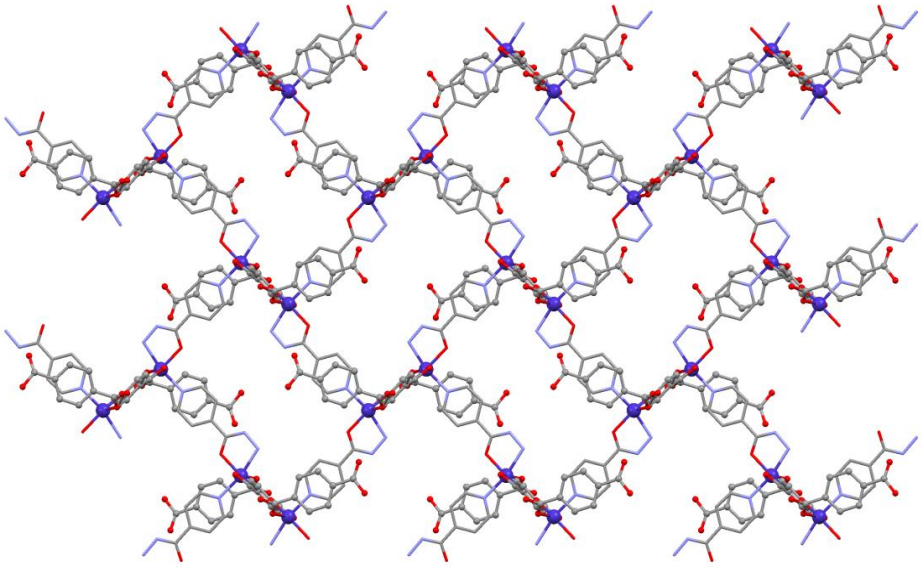

(d)

Fig. 4. 2D CPs topology: square grid in *catena*-[(μ_2-terephthalato)-(μ_2-3,3'-(hydrazine-1,2-diylidenedimethylylidene)dipyridine)-diaqua-cobalt(II)] (a) [37], rectangular grid in *catena*-((μ_4-benzene-1,4-dicarboxylato)-(μ_2-benzene-1,4-dicarboxylato)-*bis*(1-benzyl-1*H*-imidazole)-di-cobalt(II)) (b) [38], wave-like layer in *catena*-[(μ_2-benzene-1,4-dicarboxylato)-(μ_2-1,2-*bis*[2-(1*H*-1,3-imidazol-1-ylmethyl)phenoxy]ethane)-cobalt(II) dihydrate] (c) [39], and brick wall in *catena*-((μ_2-terephthalato)-*bis*(terephthalic acid)-*bis*(μ_2-isonicotinohyrazide)-di-cobalt(II)) (d) [41].

The $[Co_2(bdc)_2(L_{12})_4]_n$ crystals result from the reaction of L_{12}, $CoCl_2$, and H_2bdc acid in the presence of Et_3N in a dmf/CH_3OH solution [38]. Analysis of the crystal structure reveals a 2D network with rectangular cavities, as shown in Fig. 4b. The opposite sides of the rectangular cavity are formed by two crystallographically different bdc anions acting in different coordination modes; the metal secondary building unit (SBU) represents the binuclear cluster, $\{Co_2(COO)_4\}$.

In the extended structure of compound $\{[Co(bdc)(L_{11})]\cdot 2H_2O\}_n$ obtained under hydrothermal reaction of L_{11} with Co(II), in the presence of H_2bdc [39], the Co(II) cations are six-coordinated: each bdc^{2-}dianion acts in a bis-bidentate chelating mode to bridge the adjacent Co(II) cations to form zig-zag one-dimensional chains. These chains are linked by L_{11} ligands into a two-dimensional wave-like sheet (Fig. 4c).

If the metal ions are only coordinated with three ligand molecules giving a "T-shape" around the node, layers are formed and the motifs are referred to as honeycomb [40], brick wall [41], herringbone [42] (Fig. 4d), etc.

2.3.1.3. Three-dimensional motifs

The extension of the coordination complexes can occur in three dimensions from the nodes through the ligand connectors. The H_2bdc acid is an example of a 2-connecting ligand. For example, it has been used in the 3D motifs such as a diamondoid network, where each node is connected to four bridging ligands in a tetrahedral way, reproducing a diamond-like network. This motif has been found in the structure obtained from Co(II) ions as nodes and the H_2bdc acid, and 1,4-*bis*(2-methylbenzimidazol-1-ylmethyl)benzene (bmb) as connectors [43]. The Co(II) ion is in a distorted tetrahedral geometry defined by two nitrogen atoms of two bmb ligands and two oxygen atoms from two separated bdc^{2-} anions and the resulting structure is a threefold diamondoid framework (Fig. 5).

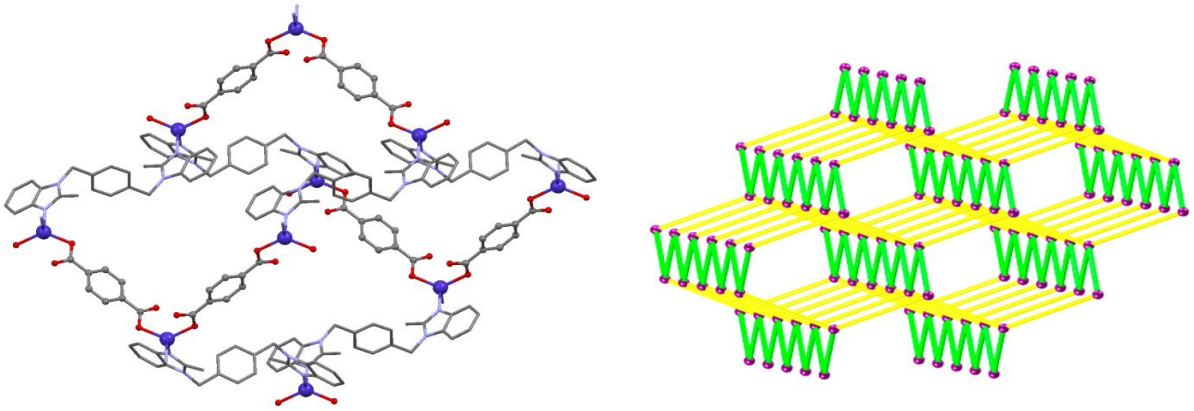

(a) (b)

Fig. 5. Perspective view of the single diamondoid net in *catena*-(*bis*(μ_2-terephthalato)-(μ_2-1,1'-(1,4-phenylenebis(methylene))-*bis*(2-methyl-1*H*-benzimidazole))-di-cobaltmonohydrate): (a) Schematic illustration of the 3D **dia** topology [43] (b).

At higher temperatures or using a longer reaction time, it is possible to obtain 3D complexes with octahedral Co(II) nodes, such as $[Co(bdc)(pyz)]_n$ (where pyz=pyrazine), where one (4,4) layer with the **sql** topology is formed with bdc dianions capping the cobalt binuclear unit, as shown in Fig. 6a (the carboxylate groups are coordinated to the cobalt ions in the equatorial sites). The pyrazine molecules are linked to the cobalt ions through the apical positions for the expansion of the structure in the third direction [44] (Fig. 6b).

A number of other three-dimensional motifs with dicarboxylic acid have been observed with different net topologies: **fcu** [45], **pcu** [46], **fsc** [47], **sra** [48], and other motifs. All of these CPs show a high stability; they present more or less large cavities filled with non-coordinating solvent molecules and/or similar networks by interpenetration.

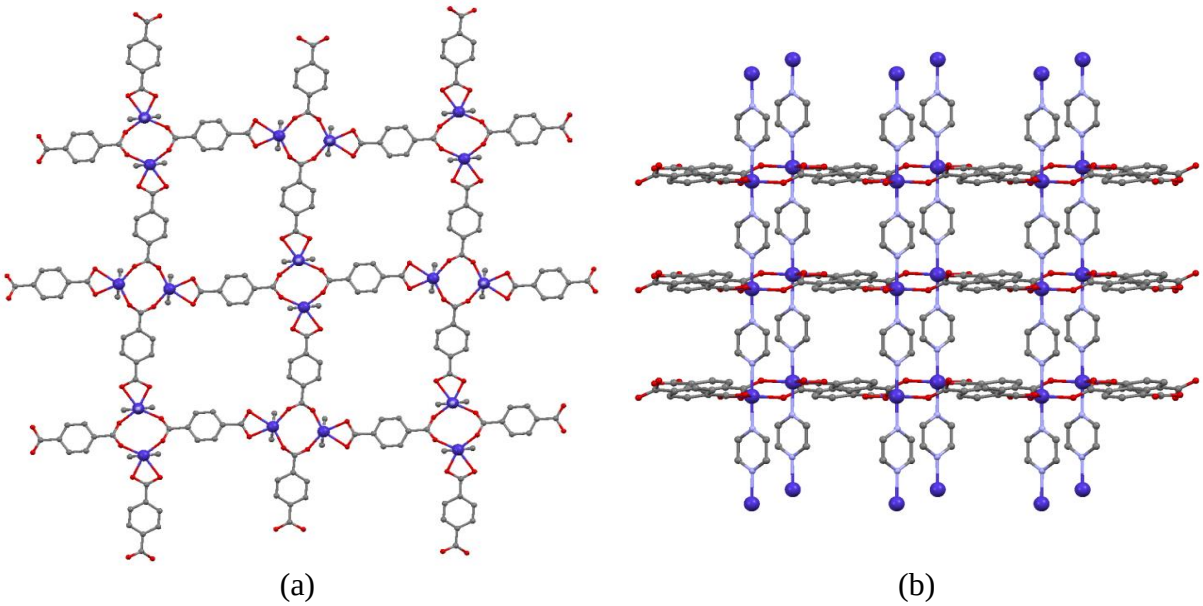

(a) (b)

Fig. 6. 3D CP $[Co(bdc)(pyz)]_n$: $\{Co(bdc)\}_n$ sheet (a) and perspective view of the three-dimensional motif [44] (b).

2.3.2. CPs of Co(II) with 4,4'-biphenyldicarboxylate

2.3.2.1. One-dimensional motifs

From the CSD search, there are three 1D CPs with an H_2bpdc ligand synthesized by the solvothermal [49] and hydrothermal [28] methods; all these compounds form a 1D zigzag chain (Table 3).

The crystal structure of $\{[Co(bpdc)(L_{37})]\cdot 1.5H_2O\}_n$ is formed by a neutral 1D zig-zag chain composed of $[Co(bpdc)(L_{37})]$ entities and free solvent disordered water molecules. The cobalt atoms are six-coordinated in a distorted $[CoN_3O_3]$ octahedral coordination environment with three carboxyl oxygen atoms from two bpdc ligands and a nitrogen atom of one L_{37} located in the basal sites and the other two nitrogen atoms from the L_{37} taken on the apical positions, as depicted in Fig. 7 [49].

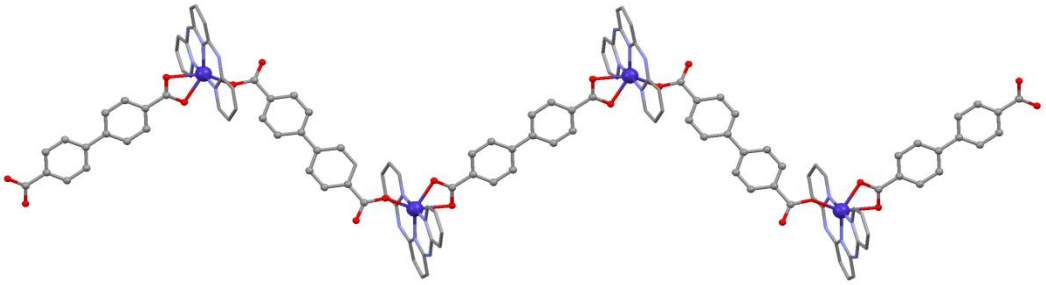

Fig. 7. 1D zig-zag polymeric chain of complex $\{[Co(bpdc)(L_{37})]\cdot 1.5H_2O\}_n$ [49].

2.3.2.2. Two-dimensional motifs

Figure 8 illustrates some of the 2D network motifs that have thus far been observed in Co(II) CPs with H_2bpdc ligand. A polyrotaxane-like network is observed in compound $[Co(bpdc)(L_{41})]_n$. This CP contains two functionally different ligands, one ligand, usually a conformationally N-donor flexible ligand, serves to assemble a molecular unit with loops, whereas the other ligand, typically a long rigid polycarboxylate, forms metal-polycarboxylate substructures (e.g., chains or sheets) and, more importantly, provides a linear rod to insert those loops [50]. The asymmetric unit of this compound consists of one Co(II) ion, one L_{41} molecule, and one $bpdc^{2-}$ anion. Each Co(II) ion is four-coordinated with distorted tetrahedral geometry composed of two carboxylic O atoms from two $bpdc^{2-}$ anions and two N atoms from two L_{41} ligands. The extension of the structure into a 2D sheet is accomplished by linear $bpdc^{2-}$ anions (Fig. 8a).

In the extended structure of compound $\{[Co(bpdc)(L_{43})_{1.5}(H_2O)](L_{43})\}_n$ obtained under hydrothermal reaction of $CoCl_2\cdot 6H_2O$, H_2bpdc, and L_{43} in distilled water and DMF, each Co(II) ion exhibits a distorted octahedral environment composed of two carboxylic O atoms from three $bpdc^{2-}$ anions and three N atoms from three L_{43} ligands and one water molecule. Each octahedral Co atom coordinates to three L_{43} ligands to form a 2D brick wall network with a (6, 3) topology (Fig. 8b) [50].

Three other 2D motifs with H_2bpdc have been observed with grid like [86, 55] and triangular grid [30] networks (Table 3).

Table 3. Selected examples for Co(II)- 4,4'-biphenyldicarboxylate CPs

Composition [a]	Method of synthesis	Color	Coordination number of Co(II)	Dimensionality	Reported properties	Reference, refcode in CSD
$\{[Co(bpdc)(L_{37})]\cdot 1.5H_2O\}_n$	solvothermal	purple	6	1D	magnetic	[70] JEXNIK
$[Co(bpdc)(HL_{38})(H_2O)]_n$	hydrothermal	red rod-like	4	1D	magnetic	[70] JEXNOQ
$\{[Co(bpdc)(L_{39})(H_2O)]\cdot nH_2O\}_n$	hydrothermal	-	6	1D	-	[28] OMEYAH
$\{[CoZn_2(bpdc)_3(dmf)_2]\cdot 4dmf\}_n$	solvothermal	purple	6	2D	-	[30] JETXAI
$[Co_2(bpdc)(L_{40})_2]_n$	stirred 5 min	blue	4	2D	-	[86] DOGMES
$[Co(bpdc)(L_{41})]_n$	hydrothermal	purple	4	2D	-	[50] MUNPIV
$\{[Co(bpdc)(L_{43})_{1.5}(H_2O)]\cdot(L_{43})\}_n$	hydrothermal	green	6	2D	-	[50] MUNPOB
$[Co(bpdc)(L_{43})]_n$	hydrothermal	blue	4	2D	-	[50] MUNPUH
$[Co(bpdc)(L_{42})]_n$	hydrothermal	blue	6	2D	fluorescence and catalytic	[87] ZORBUF
$\{[Co(bpdc)(L_{43})](dmf)_3\}_n$	solvothermal	pink	4	2D	-	[88] YARFAA
$\{[Co(bpdc)L_{44}]\cdot(EtOH)\}_n$	solvothermal	brown	6	3D	-	[89] XIHRIQ
$\{[Co_3(bpdc)_3(dma)_2]\cdot(dma)\cdot(EtOH)\}_n$	solvothermal	violet	4, 6	3D	-	[89] XIHRUC
$\{[Co_3(bpdc)_4][L_{45}]_2\cdot(CH_3OH)_2(dmf)_{1.5}\}_n$	solvothermal	purple	4, 6	3D	magnetic	[90] MOXDOT
$\{Co_3(bpdc)_4\}_n$	solvothermal	purple	6	3D	-	[91] HURGOR
$\{[Co(bpdc)(L_{46})]\cdot 2dmf\}_n$	temperature	red purple	6	3D	-	[92] IXUWII
$\{Co_3(bpdc)_3(L_{47})\}_n$	solvothermal	violet	4, 6	3D	gas-adsorption	[63] LAYGAV
$\{[Co_2(bpdc)_{1.5}(HL_{48})]\cdot dmf\cdot CH_3CN\cdot H_2O\}_n$		purple	4	3D	gas-sorption	[62] BEQFEK
$\{[Co_3(bpdc)_3(dma)_2]\cdot 4dma\}_n$	heated, 100 °C	red	6	3D	-	[56] CIFCUR
$[Co_2(bpdc)_4(L_{49})\cdot 3dmf]_n$	solvothermal	red	6	3D	-	[51] NESSOV
$\{[Co_2(bpdc)(L_{50})]\cdot dmf\}_n$	solvothermal	red	5	3D	gas-adsorption	[52] FODHUD
$\{[Co_2(bpdc)_2(H_2L_{48})]\cdot 2dmf\}_n$	solvothermal	purple	5	3D	gas-adsorption, magnetic	[53] GIYJAB
$\{[Co_2(bpdc)(HL_{51})_2]\}_n$	hydrothermal	purple	4	3D	-	[59] NOJSIQ
$\{[Co(bpdc)(L_{27})]\cdot(dmf)(H_2O)\}_n$	hydrothermal	red	6	3D	-	[93] YOVPAC
$[Co_3(bpdc)_3(L_{52})(dmf)_4]_n$	solvothermal	pink	4, 6	3D	gas adsorption	[64] LIZSOE
$\{[Co(bpdc)(L_{53})]\cdot 0.5H_2O\}_n$		red	4	3D	optical absorption	[54] WITMET
$[Co(bpdc)(L_{54})]_n$	hydrothermal	red	4	3D	fluorescence and catalytic	[55] ZORBIT
$[Co(bpdc)(L_{55})(H_2O)]_n$	hydrothermal	red	6	3D	fluorescence and catalytic	[55] ZORCAM
$\{[Co(bpdc)(HPO_4)][H_2L_{17}]\}_n$	solvothermal	blue	4	3D	-	[94] SUHMAL
$\{[Co_2(bpdc)_2(L_{56})(H_2O)]\cdot 2dma\}_n$	hydrothermal	pink	6	3D	gas sorption, magnetic	[71] VOSVAC

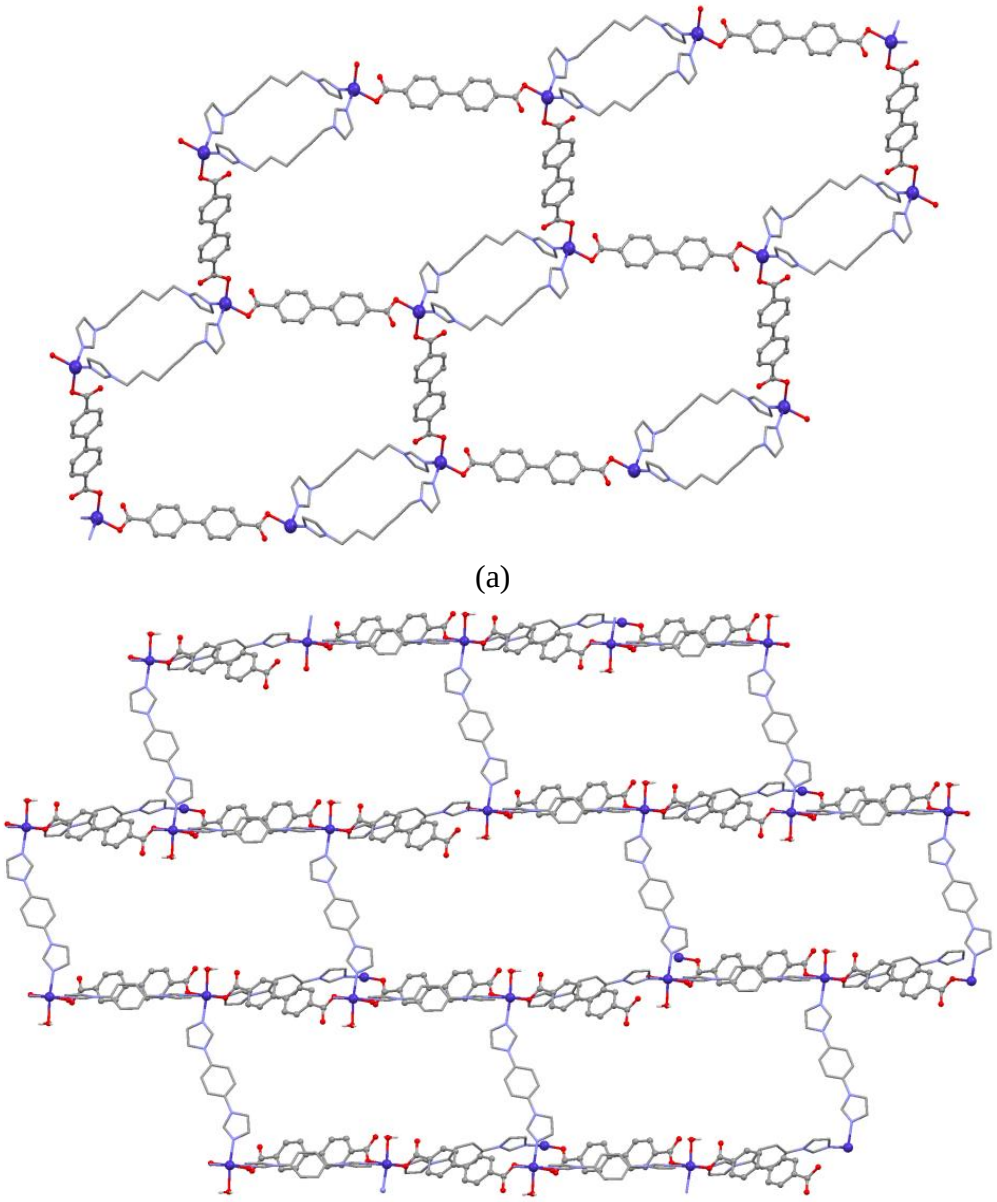

(a)

(b)

Fig. 8. 2D polyrotaxane-like network in $[Co(bpdc)(L_{41})]_n$ [50] (a); 2D brick wall net constructed from Co(II) centers and L_{43} ligands in $\{[Co(bpdc)(L_{43})_{1.5}(H_2O)](L_{43})\}_n$ (b) [50].

2.3.2.3. Three-dimensional motifs

A number of 3D motifs with H_2bpdc ligand have been observed with different net topologies, **pcu** [51-53], **rob** [54], **dia** [55], **seh** [55], **hxl** [56], **mok** [57], **hms** [58] and other motifs.

The ligands H_2bpdc and L_{51} react with the Co(II) salt to form the $\{[Co_2(bpdc)(HL_{51})_2]\}_n$ compound [59]. The asymmetric unit of this compound contains one Co(II), one partially deprotonated HL^-_{51}, and half the $bpdc^{2-}$ residue. The Co(II) ion is in a distorted tetrahedral coordination environment with three nitrogen atoms from three HL^-_{51} and one oxygen from one carboxylate group of $bpdc^{2-}$ ligand. Each HL^-_{51} coordinates with three Co(II) atoms to form a 2D network, which repeats in an ⋯ABAB⋯ stacking sequence and is further connected by $bpdc^{2-}$ ligands to form a 3D InS framework via Co(II)–O coordination interactions (Fig. 9a).

The $\{[Co(bpdc)(L_{53})]\cdot 0.5H_2O\}_n$ compound shows a **rob** organisation [54]. Its asymmetric unit consists of one crystallographically independent Co(II) ion, one L_{53} ligand, one deprotonated bpdc ligand, and half the solvent water molecule. Two crystallographically equivalent Co(II) cations are bridged by two carboxylate groups adopting a *bis*-bidentate coordination mode to generate a dinuclear Co(II) secondary building unit. The ladder chains extend in the cross direction to form a 2D network, then combine the L_{53} ligands from vertical direction to construct a 3D **rob** framework (Fig. 9b).

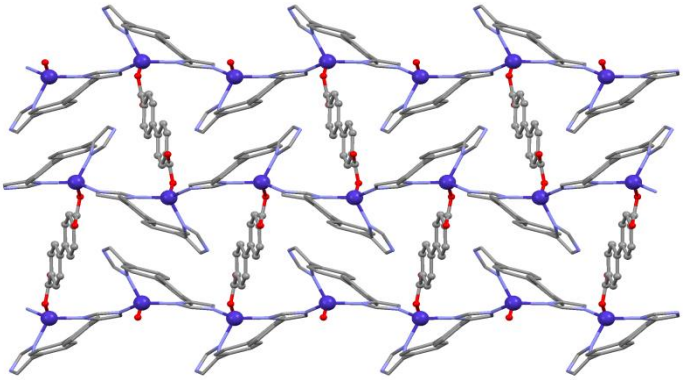

(a)

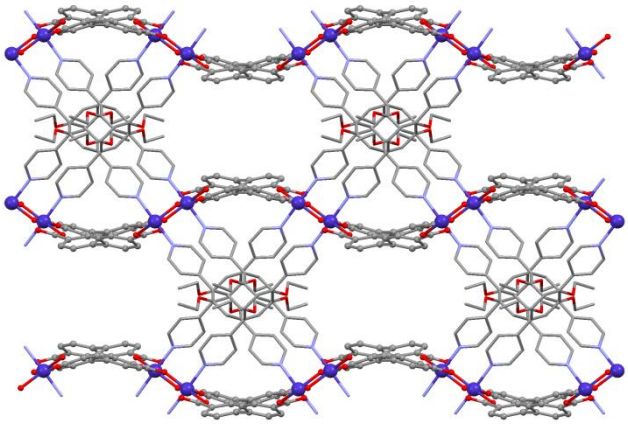

(b)

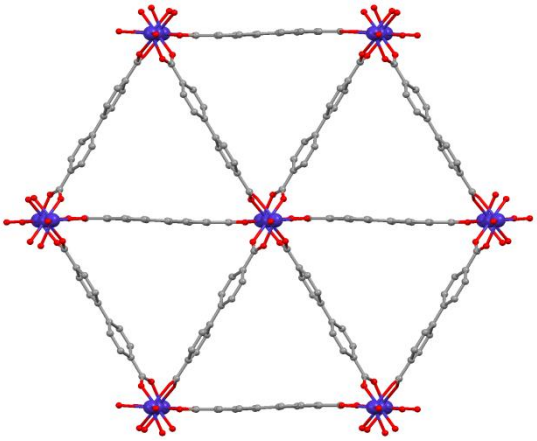

(c)

Fig. 9. 3D InS framework in $\{[Co_2(bpdc)(HL_{51})_2]\}_n$ (a) [59]; perspectives of 3D framework along the *c* axis in $\{[Co(bpdc)(L_{53})]\cdot 0.5H_2O\}_n$ (b) [54]; the **hxl** net in $\{[Co_3(bpdc)_3(dma)_2]\cdot 4dma\}_n$ (c) [56].

The $\{[Co_3(bpdc)_3(dma)_2]\cdot 4dma\}_n$ compound contains trinuclear metal centers with six coordination points; the structure adopted an **hxl** net (Fig. 9c) being assembled via the long ligand H_2bpdc [56].

3. Potential applications

The rapidly growing field of design and synthesis of CPs is attributed to their undisputable advantages as new multifunctional materials. Several examples in this part of the review reveal Co(II) MOFs with dicarboxylic ligands as promising materials for applications in gas storage, anion exchange (due to the porosity), luminescence, magnetism, and catalysis.

Gas storage is one of the possible applications for these materials. The $[Co_2(bdc)_2(L_{18})]_n$ compound has a high specific micropore volume of 0.82 cm^3g^{-1}, a hydrogen storage capacity of 2.27 wt % at −196°C and 1 bar, and an excess methane adsorption of 14.0 wt % at 30°C and 75 bar, and is a promising material for hydrogen and methane storage. The host framework shrinks upon inclusion of guest molecules and expands upon guest removal, a fascinating phenomenon in this class of materials [60]. Another example is $\{[Co_6(L_{28})(SO_4)(bdc)_2]\cdot(dmf)_7\}_n$ [61], which has ultramicropores in its structure. The dmf molecules can be removed and substituted with H_2O, methanol, and ethanol. The sorption behavior was studied for CO_2, CH_4, and N_2. The $\{[Co_2(bpdc)(L_{50})]\cdot dmf\}_n$, [52], $\{[Co_2(bpdc)_2(H_2L_{48})]\cdot 2dmf\}_n$, [53], $\{[Co_2(bpdc)_{1.5}(HL_{48})]\cdot dmf\cdot CH_3CN\cdot H_2O\}_n$ [62], and other compounds [63-65] based on positional isomeric 4,4′-biphenyldicarboxylate ligand exhibit a distinct temperature-dependent gas (CH_4, N_2, CH_4) sorption behavior.

Nowadays, MOFs have already been used for new photocatalytic materials in view of their potential applications in the green degradation of organic pollutants [66]. For example, the $\{[Co_2(bdc)(L_8)_2]\cdot 4nH_2O\}_n$ compound is an active catalyst for the degradation of orange G, rhodamine B, methylene blue, and methyl violet [67].

From a magnetic perspective, Co(II) carboxylates have shown to be potential candidates to construct molecular magnets exhibiting various bulk magnetic behavior, such as antiferromagnetism, ferromagnetism, spin canting, ferrimagnetism, and so on [68, 14]. An example of the mixed-ligand CP that well illustrates the magnetic behavior of MOFs is the $\{[Co_4(N_3)_4(bdc)_3(L_{23})_2]\cdot nH_2O\}_n$ complex [69], which reveals weak antiferromagnetic interactions between Co(II) centers. The $[Co(bpdc)(HL_{38})(H_2O)]_n$ [70] and $\{[Co(bpdc)(L_{37})]\cdot 1.5H_2O\}_n$ [70] complexes indicate weak antiferromagnetic interactions between the adjacent Co(II) (S =3/2) ions.

The widely studied Co-based MIL-53 [104] analogues, $[Co(bdc)(L_{25})]_n$ and $[Co(bdc)(L_{26})]_n$ [72, 104] show the spin canting behavior, which is attributed to the existence of a highly symmetric *trans*-$CoO_4bdcO_2L_{26}$ coordination core. There are other CPs of the Co(II) metal and an H_2bpdc ligand with magnetic properties [70, 53, 71].

4. Conclusions

Based on the data stored in the Cambridge Structural Database (CSD) and available literature sources, an attempt has been undertaken to generalize the Co(II) CPs based on two rigid dicarboxylic acid, 1,4-benzenedicarboxylic acid, and 4,4'-biphenyldicarboxylic acid. The overview covers the last-decade period of time-from 2005 to 2015-and shows how the Co(II) CP networks with dicarboxylic ligands can be built to have different dimensionalities using the rich variety of conditions and co-ligands with N-donor atoms. The extended species based on dicarboxylic aromatic acids show particularly intriguing structures for many reasons: they exhibit a large variety of distinct topologies and may serve as potentionally beneficial functional materials. The properties of these polymers range from optical to magnetic and reveal perspectives in many other fields.

Acknowledgements. The author is indebted to Dr. M.S. Fonari and Dr. L. Croitor for the fruitful discussion. The author is indebted to 14.518.02.04A project for support.

References

[1] S. R. Batten, N. R. Champness, X. M. Chen, J. Garcia-Martinez, S. Kitagawa, L. Öhrström, M. O'Keeffe, M. P. Suh, and J. Reedijk, Pure Appl. Chem., 85, 1715, (2013).

[2] (a) B. Moulton, M. J. Zaworotko, Chem. Rev., 101, 1629 (2001); (b) D. Braga, and F. Grepioni, Coord. Chem. Rev., 183,19 (1999); (c) S. Leninger, B. Olenyuk, and P. J. Stang, Chem. Rev., 100, 853, (2000); (d) L. Carlucci, G. Ciani, and D. M. Proserpio, Coord. Chem. Rev., 246, 247, (2003); (e) L. G. Beauvais and J. R. Long, Inorg. Chem., 45, 236, (2006); (f) M. Dinca, A. F. Yu, and J. R. Long, JACS, 128, 8904, (2006); (g) M. Eddaoudi, D. B. Moler, H. Li, B. Chen, T. Reineke, M. O'Keeffe, and O. M. Yaghi, Acc. Chem. Res., 34, 319, (2001); (h) O. Evans and W. Lin, Acc. Chem. Res., 35, 511, (2002); (i) M. E. Davis, Nature, 417, 813, (2002); (j) S. R. Batten and K. S. Murray, Coord. Chem. Rev., 246, 103, (2003); (k) N. L. Rosi, J. Eckert, M. Eddaoudi, D. T. Vodak, J. Kim, M. O'Keeffe, and O. M. Yaghi, Science, 300, 1127, (2003); (l) D. N. Dybtsev, H. Chun, S. H. Yoon, and K. J. Kim, Am. Chem. Soc., 126, 32, (2004); (m) O. M. Yaghi, M. O'Keeffe, N. W. Ockwig, H. K. Chae, M. Eddaoudi, and J. Kim, Nature, 423, 705, (2003).

[3] G. Q. Zhang and J. S. Ma, Cryst. Growth Des., 6, 375, (2006).

[4] (a) O. M. Yaghi and H. Li, JACS, 118, 295, (1996).

[5] (b) T. Shiga, H. Okawa, S. Kitagawa, and M. Ohba, JACS, 128, 16426, (2006).

[6] N. L. Rosi, J. Kim, M. Eddaoudi, B. Chen, M. O'Keeffe, and O. M. Yaghi, JACS, 127, 1504, (2005).

[7] (a) X. F. Wang and Y. Liu, Inorg. Chem. Commun. 27, 76 (2013); (b) A. L. Pochodylo and R. L. LaDuca, Inorg. Chem. Commun. 14, 722, (2011); (c) L. Guan, Y. H. Zhou, and H.Zhang, Inorg. Chem. Commun. 13, 737, (2010).

[8] H. Wu, W. Zhou, and Yildirim T., JACS, 131, 4995, (2009).

[9] Y. He, W. Zhou, R. Krishna, and B. Chen, ChemComm, 48, 11813, (2012).

[10] Y. S. Bae, C. Y. Lee, K. C. Kim, O. K. Farha, P. Nickias, J. T. Hupp, S. T. Nguyen, and R. Q. Snurr, Angew. Chem. Int Ed., 51, 1857, (2012).

[11] J. S. Griffith, Cambridge University Press, 1964.

[12] O. S. Wenger, Chem. Rev., 113, 3686, (2013).

[13] P. B. Lever, Elsevier, Amsterdam, (1986).

[14] M. Kurmoo, Chem. Soc. Rev., 38, 1353, (2009).

[14] (a) D. Cave, J. M. Gascon, A. D. Bond, S. J. Teat, and P. T. Wood, Chem. Commun., 10, 1050 (2002); (b) A. Distler, D. L. Lohse, and S. C. Sevov, J. Chem. Soc. DaltonTrans., 11, 1805 (1999); (c) L. Pan, N. Ching, X. Huang, and J. Li, Inorg. Chem., 39, 5333, (2000).

[16] L. E. Kreno, K. Leong, O. K. Farha, M. Allendorf, Van R. P. Duyne, and J. T. Hupp, Chem. Rev., 112, 1105, (2012).

[17] F. S. Delgado, C. A. Jimenez, P. Lorenzo-Luis, J. Pasan, O. Fabelo, L. Canadillas-Delgado, F. Lloret, M. Julve, and C. Ruiz-Perez, Cryst.Growth Des. 12, 599, (2012).

[18] (a) G. Teng, C. P. Walczak, P. J. Squattrito, D. K. Mohanty, W. Schare, M. R. Giolando, and K. Kirschbaum, Acta Crystallogr., Sect.C: Cryst. Struct. Commun. 65, 76, (2009); (b) J. Wang, X. Jing, Y. Cao, G. Li, Q. Huo, and Y. Liu, CrystEngComm 17, 604, (2015), (c) X. Hua, W. Li, Y. Xu, J. Wu, and W. H. Xuebao (Chin.) (Acta Phys.-Chim.Sin) 28, 1815, (2012); (d) K. Shankar, B. Das, and J. B. Baruah, Eur. J. Inorg. Chem. 2013, 6147, (2013).

[19] C. R. Groom and F. H. Allen, Angew.Chem.Int.Ed., 53 , 662, (2014).

[20] (a) J. He, C. Yang, Z. Xu, M. Zeller, A. D. Hunter, and J. Lin, J. Solid State Chem. 182, 1821, (2009); (b) J. Zhang, L. Wojtas, R. W. Larsen, M. Eddaoudi, and M. J. Zaworotko, JACS 131, 17040, (2009).

[21] S. Q. Wei, X. H. Yin, C. W. Lin, C. J. He, and H. B. Ou, University of Edinburgh, (2013).
[22] (a) H. B. Xu, Z. M. Su, K. Z. Shao, Y. H. Zhao, Y. Liang, and Y. C. Zhang, Inorg. Chem. Commun. 7, 260 (2004); (b) J. Cano, G. De Munno, J. L. Sanz, R. Ruiz, J. Faus, F. Lloret, M. Julve, and A. Caneschi, J. Chem. Soc. Dalton Trans, 67., 1915, (1997).
[23] (a) S. Kitagawa and S. Noro, Compreh. Coord. Chem. 7, 231 (2004); (b) W. Clegg, Compreh. Coord. Chem. 1, 579, (2004).
[24] (a) T. Panda, P. Pachfule, and R. Banerjee, Chem. Commun., 47, 7674 (2011); (b) G. T. Vuong, M. H. Pham, and T. O. Do, Dalton Trans., 42, 550, (2013).
[25] (a) Q. Liu, L. L. Yu, Y. Wang, Y. Z. Ji, J. Horvat, M. L. Cheng, X. Y. Jia, and G. X. Wang, Inorg. Chem., 52, 2817, (2013); (b) J. J. Gassensmith, J. Y. Kim, J. M. Holcroft, O. K. Farha, J. F. Stoddart, J. T. Hupp, and N. C. Jeong, J. Am. Chem. Soc., 136, 8277, (2014).
[26] (a) Z. J. Zhang, L. P. Zhang, L. Wojtas, P. Nugent, M. Eddaoudi, and M. J. Zaworotko, JACS, 134, 924 ,(2012); (b) M. Saito, T. Toyao, K. Ueda, T. Kamegawa, Y. Horiuchi, and M. Matsuoka, Dalton Trans., 42, 9444, (2013).
[27] X. M. Chen and M. L. Tong, Acc. Chem. Res., 40, 162, (2007).
[28] C. Y. Sun, B. Dong, Q. Lv, and X.-J. Zheng, Z. Anorg. Allg. Chem. 637, 276, (2011).
[29] L. G. Zhu and H. P. Xiao, Z. Anorg. Allg. Chem., 634, 845, (2008).
[30] Y. Wang, B. Bredenkotter, B. Riegera, and D. Volkmer, Dalton Trans., 689, (2007).
[31] R. A. Coxall, S. G. Harris, D. K. Henderson, S. Parsons, P. A. Tasker, and R. E. P. Winpenny, Dalton Trans., Harris notation describes the binding mode as [X.Y1Y2Y3 ...Yn], where X is the overall number of metals bound by the whole ligand, and each value of Y refers to the number of metal atoms attached to the different donor atoms. 2349, (2000).
[32] C. F. Macrae, P. R. Edgington, P. McCabe, E. Pidcock, G. P. Shields, R. Taylor, M. Towler, and J. Van de Streek, J. Appl. Cryst., 39, 453, (2006).
[33] X. H. Chen, H. Huang, M. X. Yang, L. J. Chen, and S. Lin, ActaCrystallogr., Sect. C: Cryst. Struct. Chem., 70, 488, (2014).
[34] S. Q. Wei, X. -H. Yin, C. W. Lin, C. J. He, and H. -B. Ou, Synth. React. Inorg., Met.Org., Nano-Met. Chem., 43, 580, (2013).
[35] S. C. Manna, E. Zangrando, J. Ribas, and N. R. Chaudjuri, Dalton Trans., 1383, (2007).
[36] X. M. Liu, R. B. Lin, J. P. Zhang, and X. M. Chen, Inorg. Chem., 51, 5686, (2012).
[37] J. Zhou, L. Du, Y. F. Qiao, Y. Hu, B. Li, L. Li, X. Y. Wang, J. Yang, M. J. Xie, and Q. H. Zhao, Cryst. Growth Des., 14, 1175, (2014).
[38] Q. X. Liu, X. J. Zhao, X. M. Wu, S. W. Liu, Y. Zang, S. S. Ge, Wang X.G., and J. H. Guo, Inorg. Chem. Commun., 11, 809, (2008).
[39] N. N. Yuan, Q. K. Liu, J. P. Ma, R. Q. Huang, and Y. B. Dong, ActaCrystallogr., Sect. C: Cryst.Struct. Commun., 67, 119, (2011).
[40] Y. Sun, S. Liu, Y. Xu, L. Wu, D. Gao, G. Zhang, and D. Z. Liao, Polyhedron, 74, 39, (2014).
[41] G. P. Yong, Y. Z. Li, C. F. Li, Y. M. Zhang, and W. L. She, Dalton Trans., 40, 4131, (2011).
[42] F. B. De Almeida, F. H. Silva, M. I. Yoshida, H. A. De Abreu, and R. Diniz, Inorg. Chim. Acta, 402, 60, (2013).
[43] Q. Guo, C. Xu, B. Zhao, Y. Jia, H. Hou, and Y. Fan, Cryst. Growth Des., 12, 5439, (2012).
[44] A. Abbasi, S. Tarighi, and A. Badiei, Transition Met. Chem., 37, 679, (2012).
[45] S. A. Kumalah, M. V. L. Mempin, A. J. Cairns, and K. T. Holman, J. Am. Chem. Soc. 133, 1634, (2011).

[46] H. J. Lee, P. Y. Cheng, C. Y. Chen, J. S. Shen, D. Nandi, and H. M. Lee, CrystEngComm 13, 4814, (2011).
[47] J. Xu, X. Q. Yao, L. F. Huang, Y. Z. Li, and H. G. Zheng, CrystEngComm 13, 857, (2011).
[48] A. S. Munn, G. J. Clarkson, F. Millange, Y. Dumont, and R. I. Walton, CrystEngComm, 15, 9679, (2013)
[49] L. J. Zhou, Y. Y. Wang, C. H. Zhou, C. J. Wang, Q. Z. Shi, and S. M. Peng, Cryst.Growth Des. 7, 300, (2007).
[50] Y. Liu, Y. Qi, Y. Y. Lv, Y. X. Che, and J. M. Zheng, Cryst.Growth Des. 9, 4797, (2009).
[51] X. R. Hao, G. -S. Yang, K. -Z. Shao, Z. M. Su, G. Yuan, and X. L. Wang, J. Solid State Chem. 198, 143, (2013).
[52] B. Liu, J. Shi, K. -F. Yue, D. S. Li, and Y. Y. Wang, Cryst. Growth Des. 14, 2003, (2014).
[53] L. N. Jia, Y. Zhao, L. Hou, L. Cui, H. H. Wang, and Y. Y. Wang, J. Solid State Chem. 210, 251, (2014).
[54] C. Zhang, M. Zhang, L. Qin, and H. Zheng, Cryst. Growth Des. 14, 491, (2014)
[55] X. X. Wang, B.Yu, K. V. Hecke, and G. H. Cui, RSC Advances 4, 61281, (2014).
[56] S. Y. Yang, H. B. Yuan, X. B. Xu, and R. B. Huang, Inorg.Chim.Acta 403, 53, (2013)
[57] Y. Gong, Y. C. Zhou, T. F. Liu, J. Lu, Proserpio D.M., and Cao R., ChemCommun. 47, 5982, (2011).
[58] Q. Chen, Y. Y. Jia, Z. Chang, T. T. Wang, B. Y. Zhou, R. Feng, and X. H. Bu, Cryst.Growth Des. 14, 5189, (2014).
[59] K. Chen, Y. -S. Kang, L. Luo, Y. Zhao, P. Wang, L. Qing, Y. Lu, and W. -Y. Sun, Polyhedron 79, 239, (2014).
[60] H. Wang, J. Getzschmann, I. Senkovska, and S. Kaskel, Microporous and Mesoporous Mater. 116, 653, (2008)
[61] Q. Chen, Z. Chang, W. C. Song, H. Song, H. B. Song, T. L. Hu, and X. H. Bu, Angew. Chem., Int. Ed., 52, 11550, (2013).
[62] L. Hou, L. N. Jia, W. J. Shi, L. Y. Du, J. Li, Y. Y. Wang, and Q. Z. Shi, Dalton Trans. 42, 6306, (2013).
[63] L. Schlechte, V. Bon, N. Klein, R. Grunker, N. Klein, I. Senkovska, and S. Kaskel, Polyhedron 44, 179, (2012)/
[64] J. T. Shi, K. F. Yue, B. Liu, C. S. Zhou, Y. L. Liu, Z. G. Fang, and Y. Y. Wang, CrystEngComm 16, 3097, (2014).
[65] S. T. Zheng, X. Zhao, S. Lau, A. Fuhr, P. Feng, and X. Bu, JACS 135, 10270, (2013
[66] (a) H. Qu, L. Qiu, X. K. Leng, M. M. Wabg, S. M. Lan, L. L. Wen, and D. F. Li, Inorg. Chem. Commun., 14 1347-1351, (2011); (b) Lin H.S. and Maggard P.A., Inorg. Chem., 47 8044, (2008); (c) Liao Z.L., Li G.D., Bi M.H., and hen J.S., Inorg. Chem., 47, 4844, (2008).
[67] H. Y. Sun, C. B. Liu, Y. Cong, M. H. Yu, H. Y. Bai, and G. B. Che, Inorg. Chem. Commun., 35, 130, (2013).
[68] F. P. Huang, J. L. Tian, W. Gu, X. Liu, S. P. Yan, D. Z. Liao, and P. Cheng, Cryst. Growth Des., 10, 1146, (2010).
[69] S. H. Wang, F. K. Zheng, M. F. Wu, Z. F. Liu, J. Chen, Y. Xiao, R. Li, and G. C. Guo, Cryst. Eng. Comm., 16, 2009, (2014).
[70] L. J. Zhou, Y. Y. Wang, C. H. Zhou, C. J. Wang, Q. Z. Shi, and S. M. Peng, Cryst.Growth Des. 7, 300, (2007).
[71] M. X. Zheng, X. -J. Gao, C. L. Zhang, L. Qin, and H. G. Zheng, Dalton Trans. 44, 4751, (2015)
[72] A. S. Munn, G. J. Clarkson, F. Millange, Y. Dumont, and R. I. Walton, CrystEngComm, 15, 9679, (2013).

[73] C. Hou, Y. Zhao, and W. Y. Sun, Inorg. Chem. Commun., 39, 126, (2014).
[74] D. Liu, Y. Liu, G. Xu, G. Li, Y. Yu, and C. Wang, Eur. J. Inorg. Chem., 2012, 4413, (2012).
[75] Y. H. Wang, Y. W. Li, W. L. Chen, Y. G. Li, and E. B. Wang, J. Mol. Struct., 877, 56, (2008).
[76] J. S. Hu, Y. J. Shang, X. Q. Yao, L. Qin, Y. Z. Li, Z. J. Guo, H. G. Zheng, and Z. L. Xue, Cryst. Growth. Des., 10, 4135, (2010).
[77] P. Z. Li, X. M. Lu, and X. Z. Yang, Inorg. Chim. Acta, 361, 293, (2008).
[78] D. K. Maity, B. Bhattacharya, R. Mondal, and D. Ghoshal, Cryst. Eng. Comm., 16, 8896, (2014).
[79] B. Bhattacharya, D. Maity, P. Pachfule, and D. Ghoshal, Inorg. Chem. Front., 1, 414, (2014).
[80] Z. Q. Shi, Z. J. Guo, and H. G. Zheng, Dalton Trans., 43, 13250, (2014).
[81] J. S. Goldsworthy, A. L. Pochodyl, and R.L. LaDuca, Inorg. Chim. Acta, 419, 26, (2014).
[82] L. Qin, X. H. Zheng, S. L. Xiao, and G. H. Cui, Transition Met. Chem., 38, 891, (2013).
[83] Y. T. Yang, F. H. Zhao, Y. X. Che, and J. M. Zheng, Inorg. Chem. Commun., 14, 1802, (2011).
[84] W. G. Yuan, F. Xiong, H. L. Zhang, W. Tang, S. F. Zhang, Z. He, L. H. Jing, and Qin D.B., CrystEngComm, 16, 7701, (2014).
[85] Y. Gong, M. M. Zhang, P. Zhang, H. F. Shi, P. G. Jiang, and J. H. Lin, CrystEngComm, 16, 9882, (2014).
[86] G. A. Santillan and C. J. Carrano, Inorg.Chem. 47, 930, (2008).
[87] X. X. Wang, B. Yu, K. V. Hecke, and G. H. Cui, RSC Advances 4, 61281, (2014).
[88] X. Z. Song, S. -Y. Song, C. Qin, S. Q. Su, S. N. Zhao, M. Zhu, Z. M. Hao, and H. J. Zhang, Cryst. Growth Des. 12, 253, (2012).
[89] S. H. Kim, H. S. Huh, and S. W. Lee, J. Mol. Struct. 841, 78, (2007).
[90] F. Luo, Y. X. Che, and J. M. Zheng, Cryst. Growth Des. 9, 1066, (2009).
[91] Y. Du, A. L. Thompson, and D. O'Hare, Dalton Trans. 39, 3384, (2010).
[92] Y. Gong, Y. C. Zhou, T. F. Liu, J. Lu, D. M. Proserpio, and R. Cao, ChemCommun. 47, 5982, (2011).
[93] Q. Chen, Y. Y. Jia, Z. Chang, T. T. Wang, B. Y. Zhou, R. Feng, and X. H. Bu, Cryst.Growth Des. 14, 5189, (2014).
[94] Q. -R. Ding, L. M. Li, L. Zhang, and J. Zhang, Inorg.Chem. 54, 1209, (2015).
[95] X. X. Wang, Y. J. Ma, H. H. Li, and G. H. Cui, Transition Met.Chem. 40, 99, (2015).
[96] J. Y. Lee, J. Y. Lee, and H. M. Lee, Inorg.Chem.Commun. 52, 16, (2015).
[97] M. Bagherzadeha, F. Ashouri, and M. Dakovic, J. Solid State Chem. 223, 32, (2015).
[98] Y. Wang, Y. Qi, Q. Li, Z. Lv, and Y. Wang, Polyhedron, 85, 389, (2015).
[99] A. S. Munn, S. Amabilino, T. W. Stevens, L. M. Daniels, G. J. Clarkson, F. Millange, M. J. Lennox, T. Duren, S. Bourelly, P. L. Llewellyn, and R. I. Walton, Cryst. Growth Des., 15 (2), 891, (2015).
[100] W. J. Huang, C. J. Hsu, S. K. Tsai, H. Y. He, J. J. Ding, T. W. Hsu, C. C. Yang, and J. D. Chen, RSC Advances 5, 23374, (2015).
[101] F. P. Huang, C. Yang, H. Y. Li, P. F. Yao, X. H. Qin, S. P. Yan, and M. Kurmoo, Dalton Trans. 44, 6593, (2015).
[102] Z. X. Li, G. Ye, J. Han, Y. Yang, K. Y. Zou, X. Wang, X. L. Wang, and X. F. Gou, Dalton Trans. 44, 9209 ,(2015).
[103] J. P. Meng, Y. Gong, Q. Lin, M. M. Zhang, P. Zhang, H. F. Shi, and J. H. Lin, Dalton Trans. 44, 5407, (2015).
[104] C. Serre, F. Millange, C. Thouvenot, M. Noguès, G. Marsolier, D. Louër, and G. Férey, JACS, 124 (45), 13519, (2002).